medRxiv preprint doi: https://doi.org/10.1101/2020.04.30.20083568; this version posted May 12, 2020. The copyright holder for this preprint (which was not certified by peer review) is the author/funder, who has granted medRxiv a license to display the preprint in perpetuity. It is made available under a CC-BY-NC-ND 4.0 International license .

The geography of COVID-19 spread in Italy and implications for the relaxation of confinement measures

Enrico Bertuzzo[1,2], Lorenzo Mari[3], Damiano Pasetto[1], Stefano Miccoli[4], Renato Casagrandi[3], Marino Gatto[3], and Andrea Rinaldo[5,6]

[1]Dipartimento di Scienze Ambientali, Informatica e Statistica, Università Ca' Foscari Venezia, 30172 Venezia-Mestre IT
[2]Science of Complexity Research Unit, European Centre for Living Technology, 30123 Venice IT
[3]Dipartimento di Elettronica, Informazione e Bioingegneria, Politecnico di Milano, 20133 Milano IT
[4]Dipartimento di Meccanica, Politecnico di Milano, 20156 Milano IT
[5]Laboratory of Ecohydrology, École Polytechnique Fédérale de Lausanne, 1015 Lausanne CH
[6]Dipartimento ICEA, Università di Padova, 35131 Padova IT

We examine the spread of Severe Acute Respiratory Syndrome Coronavirus 2 (SARS-CoV-2) in Italy, to address the appropriate methodological choices for the design of selective relaxations of the current containment measures. Pressing relevance stems from the need to restart the economy dramatically affected by the lockdown. We employ a spatially explicit, data-intensive model of the patterns of disease spread in Italy, which devotes proper attention to the paramount role of inapparent infections. We aim at providing tools to: estimate the baseline trajectory, i.e. the expected unfolding of the outbreak if the current containment measures were kept in place indefinitely; assess possible deviations from the baseline, should relaxations of the current lockdown result in increased disease transmission; and estimate the isolation effort required to prevent a resurgence of the outbreak. A $40\,\%$ increase in effective transmission as a result of the loosening of confinement measures would yield an epidemic curve that shows a major rebound, larger than the previous peaks in most regions. A control effort capable of isolating a daily percentage of approximately $5.5\,\%$ of the exposed and highly infectious individuals proves necessary to counterbalance such an increase and maintain the epidemic curve onto the decreasing baseline trajectory. We explore several scenarios, provide the basic data to design the related control strategies, and discuss their feasibility. Should suitable control via tracing and testing prove unfeasible, stop-and-go enforcement or delay of the lockdown relaxations would be necessary to reduce the isolation effort required to maintain the epidemic trajectory under control.

NOTE: This preprint reports new research that has not been certified by peer review and should not be used to guide clinical practice.

medRxiv preprint doi: https://doi.org/10.1101/2020.04.30.20083568; this version posted May 12, 2020. The copyright holder for this preprint (which was not certified by peer review) is the author/funder, who has granted medRxiv a license to display the preprint in perpetuity. It is made available under a CC-BY-NC-ND 4.0 International license .

Introduction

While the pandemic caused by SARS-CoV-2 is still ravaging most countries of the world[1,2] and containment measures are implemented worldwide[3], a debate is emerging on whether these measures might be partially alleviated, and in case how and when[4–7]. This discussion requires appropriate models that guide decision-makers through alternative actions via scenarios of the related trajectories of the epidemic.

The setup of country-wide epidemiological models[8,9] is particularly challenging for SARS-CoV-2 owing to inapparent infections[10–12] and to the marked spatial heterogeneity of the epidemic spread[9]. For example, in Italy, where the (largely underestimated) reported infections and deaths are respectively 207 428 and 28 236 as of May 1, the latitudinal characters of the spread of infections showed marked delays in the beginning of the local outbreaks[9].

To make things even more complicated, empirical evidence suggests that asymptomatic infectious individuals could be as contagious as symptomatic ones[10,13]. Pre-symptomatic infectious cases are also an important vehicle of infection, as epitomized by the value of the pre-symptomatic transmission parameter which proves larger than the transmission rates of symptomatic and asymptomatic infections[9]. This is supported by field epidemiological evidence[14–16] and virological findings reporting cases of COVID-19 fueled by strong pre- or oligo-symptomatic transmission[17–19] and shedding[20].

We base our analysis on a recently published, spatially explicit model of the COVID-19 spread in Italy, inclusive of mobility among communities, the timing of infection seeding, mobility restrictions and social distancing[9]. We assume that, for the time being and in the near-term, no imported infections occur from outside the national boundaries. The model is a spatial system of coupled ordinary differential equations that solves in time, and for each of the 107 Italian provinces, the balance of, and the coupled fluxes among, several epidemiological compartments in which the total population of a community is subdivided. Specifically, we describe the dynamics of individuals who are susceptible, latently infected, at peak infectivity, asymptomatic/mildly symptomatic, infected with heavy symptoms, and recovered (Methods). Local communities are connected by mobility fluxes of individuals from the mobile epidemiological compartments (susceptible, exposed, peak infectivity, asymptomatic/mildly symptomatic and recovered individuals). Thus, the force of infection of each community (Methods) depends not only on the local epidemiological variables, but also on those of the connected communities. Infections, therefore, not only do occur within each community, but can also be imported from, or exported to, linked communities. In addition, the model accounts for infections occurring because individuals of different communities meet in a third location. The relative balance of the fluxes among the various compartments is regulated by process parameters that are estimated in a Bayesian framework (Methods).

The fundamental improvements of our framework with respect to other non-spatial, well-mixed models initially devised for single megacities[21], or for a whole country[22], lie

medRxiv preprint doi: https://doi.org/10.1101/2020.04.30.20083568; this version posted May 12, 2020. The copyright holder for this preprint (which was not certified by peer review) is the author/funder, who has granted medRxiv a license to display the preprint in perpetuity. It is made available under a CC-BY-NC-ND 4.0 International license .

in the detailed description of the geographic context and its networks of epidemiological interactions. Therefore, we have updated the benchmark model[9] through the estimation of parameters using the number of daily hospitalized cases in all 107 Italian provinces from February 24 to May 1 (Methods). To estimate parameters, we account for the set of progressively more restrictive measures that were introduced from February 22 (initial restrictive measures) to March 22, when Italy went into a full lockdown closing also non-essential industrial and other production activities.[23–25].

Available epidemiological data[26–28] must be viewed as an approximation. In fact, confirmed infections depend on testing efforts that local officials were able to deploy to identify confirmed infections, thus leading to underreporting. The ratio of confirmed to actual infections was estimated to be around 10%[9]. Under-reporting applies even to fatality counts, although to a lesser extent with respect to reported infections[29,30]. Moreover, fatality rate can change in time due to stress in health care facilities [30]. In order to alleviate these problems, in this work we used for parameter estimation only reconstructed data on daily rates of hospitalization (Methods).

Health-policy and science underpin the design of suitable containment strategies, which include individual and collective (local and medium- to long-distance) mobility limitations[23], provision of personal protective equipment (PPE)[31], massive, possibly targeted identification of infectious cases[32,33], and the setup of layers of administrative and environmental engineering controls[31]. These strategies must consider the level of connectivity realized among communities after lockdown release, and the different epidemiological parameters that effectively characterize them[8,9]. Recent results on the effects of lifting restrictions in the Boston area suggest that a response system based on enhanced contact tracing and testing can play a major role in relaxing social distancing interventions in the absence of herd immunity against SARS-CoV-2[34].

Here, we generate scenarios of the Italian infection dynamics resulting from the bulk effect of lifting the current restrictions, which initiated on May 4. How will the modes of relaxation of previous confinement measures affect residual epidemic trajectories? The answer to this question is not trivial, because different activities will be allowed to resume at different times. In addition, acquired awareness may have different lasting effects on social behaviour regardless of imposed measures, and compliance to proper use of PPE[31] may fade away in time. Here, we propose to assess the actual increase in overall transmission by tracking the departure of the epidemic curve from the one projected by using the transmission rate achieved during the lockdown. We address the mitigation of the likely increased exposure, in particular by estimating the sufficient number of case isolation interventions that would prevent rebounding of the epidemics.

medRxiv preprint doi: https://doi.org/10.1101/2020.04.30.20083568; this version posted May 12, 2020. The copyright holder for this preprint (which was not certified by peer review) is the author/funder, who has granted medRxiv a license to display the preprint in perpetuity. It is made available under a CC-BY-NC-ND 4.0 International license .

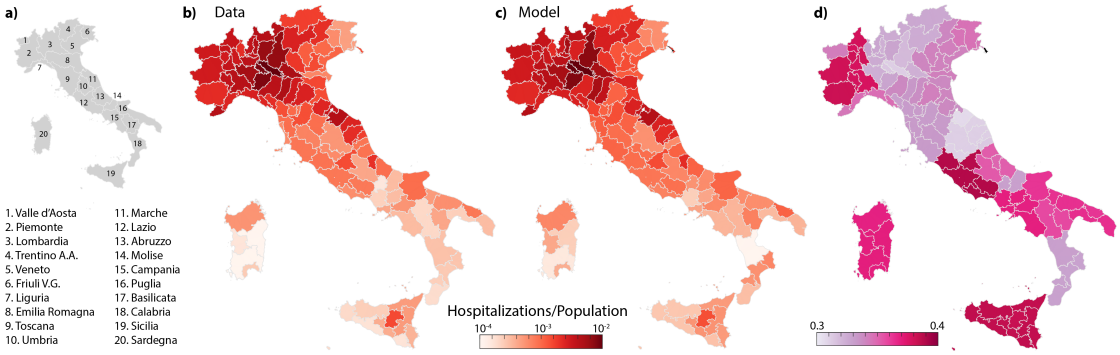

Figure 1: Comparative analysis of data and model results for hospitalizations in 107 Italian provinces as of May 1, 2020. The maps show: a) a sketch of the Italian regions; b, c) the prevalence of cumulative hospitalizations in each Italian province up to May 1, reconstructed data (b) and model simulations (c); d) Ratio between the estimated transmission rate on May 1, and the one estimated at the beginning of the outbreak (February 24).

Results

Parameter estimation and model results

The model reproduces well the prevalence of cumulative hospitalizations in the 107 Italian provinces up to May 1 (Figs. 1 and 2). By considering heterogeneous transmission rates after March 22 (see Methods), we estimate a large reduction in the effective disease transmission rate in each province. This reduction, expressed as a ratio of effective transmission estimated on May 1 to the initial uncontrolled one, ranges between 0.3 and 0.4 depending on location (Fig. 1d). Technically, this reduction is computed via the product of the reduction in transmission rates (β_{P_3}/β_{P_0}, see Methods) times the fraction of the population still susceptible to the infection on May 1. The latter, however, is very sensitive to the fraction of infections that develop heavy symptoms (parameter σ in the model, see Methods). The reference value assumed is σ=25%, which is consistent with empirical evidence[8]. However, we carried out a sensitivity analysis to investigate the role of inapparent infections[10] by repeating parameter estimation with σ=10% and 50% as well, thus covering a broad enough spectrum of possible values. All other parameters, whose meaning is detailed in the Methods Section, are reported in Table 1.

Scenarios of national and regional epidemic trajectories

If the transmission rates estimated at the end of the lockdown persisted indefinitely, the epidemic curve would continue to decrease in all Italian regions (baseline scenario, blue curve in Fig. 2), although at different rates. We report for convenience daily hospital-

medRxiv preprint doi: https://doi.org/10.1101/2020.04.30.20083568; this version posted May 12, 2020. The copyright holder for this preprint (which was not certified by peer review) is the author/funder, who has granted medRxiv a license to display the preprint in perpetuity. It is made available under a CC-BY-NC-ND 4.0 International license .

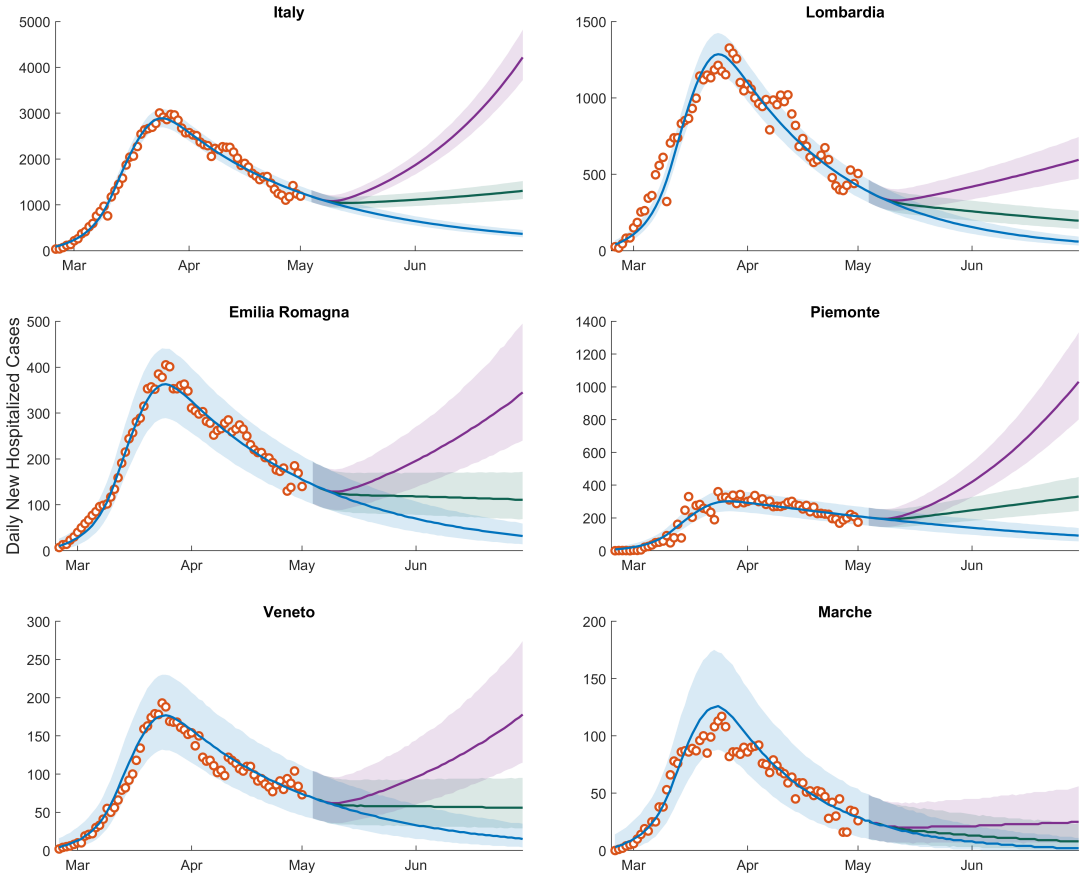

Figure 2: Daily numbers of newly hospitalized cases for Italy and its hardest hit regions. Shown here are reconstructed data (empty circles), and model results (solid lines and confidence intervals). Clockwise from top: Italy, Lombardia, Piemonte, Marche, Veneto and Emilia Romagna. The remaining regions are shown in Fig. S1. The blue solid line represents the baseline scenario, i.e. the median of the computed results with current restriction measures maintained indefinitely beyond May 3, 2020. The green and purple solid lines represent the scenarios corresponding to a release of the containment measures determining an effective increase in the overall transmission rates of respectively 20 % and 40 %. The 95 % confidence intervals are color-coded in analogy to their median scenarios. Plots refer to a fraction of infections leading to heavy symptoms σ equal to 25%. Plots referring to the other two values considered (σ=50% and 10%) are reported in Supplementary Figures S2 and S3.

medRxiv preprint doi: https://doi.org/10.1101/2020.04.30.20083568; this version posted May 12, 2020. The copyright holder for this preprint (which was not certified by peer review) is the author/funder, who has granted medRxiv a license to display the preprint in perpetuity. It is made available under a CC-BY-NC-ND 4.0 International license .

ization counts aggregated for administrative regions, although the model accounts for a finer spatial granularity (107 provinces and metropolitan areas, see Fig. 1).

The lockdown in Italy has been relaxed on May 4. Here, we propose to assess the actual increase in overall transmission of the infection by tracking the departure of the residual epidemic curve from the baseline scenario. This allows us to estimate the overall effect of the new exposure caused by the local lockdown relaxations. An increase of 20 % in the transmission rate, subsumimg the effective combination of economic activities' resumption and modified contact rates, yields a decline milder than that of the baseline for the new daily hospitalization cases in most Italian regions. A 40 % increase would instead determine a significant rebound of the epidemic in most regions (Fig. 2, see also Supplementary Information (SI)).

The trajectories shown in Fig. 2 prove robust with respect to the assumed value of σ, at least for the relatively short projection horizons considered here, which are relevant to contingency planning. Indeed, the curves in Fig. 2, obtained with $\sigma = 25\%$, compare well with those reported in Supplementary Figures S2 and S3, obtained by assuming $\sigma = 50\%$ and 10%, respectively.

The fraction of susceptible individuals obtained for different values of σ, the heavy symptomatic fraction, strongly varies throughout the Italian regions (Fig. 3). Since the beginning of the epidemic up to May 1, the susceptible fraction of the population has decreased more markedly in the northern regions, which have been more severely hit by the outbreak, with the minimum values reached in Lombardia (0.97, 0.95, and 0.87 with σ=50, 25 and 10%, respectively). By contrast, central and southern regions had minimal reductions of their susceptible fraction. These results bear obvious implications on possible revamping of the epidemics reaching new peaks of dangerous proportions, as it denies any short- or medium-term possibilities to attain herd immunity.

Different assumptions for σ result in different values of the infection fatality rate (IFR), defined as the ratio between the official death count (at a certain date) and the corresponding total number of infections estimated by the model. As of May 1, we estimate an IFR of 4, 2 and 0.8%, respectively for $\sigma = 50$, 25 and 10%.

Isolation effort

Isolation of cases to counterbalance the possible increase in transmission following the relaxation of the restrictive measures is a conceivable strategy, alternative to extending lockdown or to stop-and-go enforcement of containment measures. Isolation effort critically depends on tracing and testing. Evidence of peak of viral shedding before and right after symptom onset[13] (see also Methods) suggests that isolation is more effective if targeted at incubating individuals, i.e. those in the exposed, E, and peak of infectivity, P, compartments of the model. We therefore focus on these individuals and estimate the percentage and the corresponding number of individuals that should be isolated daily (Fig. 4, Methods) to counterbalance the increase in transmission resulting from

medRxiv preprint doi: https://doi.org/10.1101/2020.04.30.20083568; this version posted May 12, 2020. The copyright holder for this preprint (which was not certified by peer review) is the author/funder, who has granted medRxiv a license to display the preprint in perpetuity. It is made available under a CC-BY-NC-ND 4.0 International license .

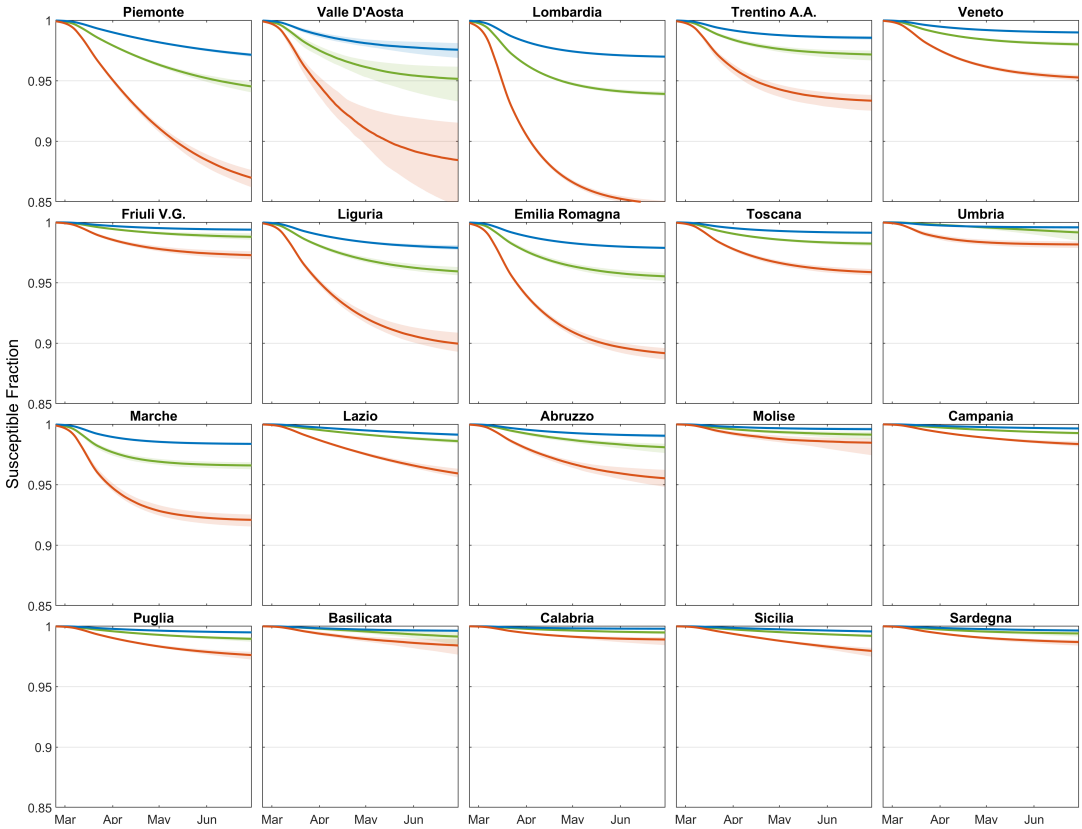

Figure 3: Temporal dynamics of the fraction of susceptible individuals in each region, estimated by considering three possible percentages of heavy symptomatic infections: $\sigma = 50\,\%$ (blue curve), $25\,\%$ (green curve), and $10\,\%$ (red curve). Thick solid curves refer to medians values, while shaded areas indicate the 95% confidence intervals.

medRxiv preprint doi: https://doi.org/10.1101/2020.04.30.20083568; this version posted May 12, 2020. The copyright holder for this preprint (which was not certified by peer review) is the author/funder, who has granted medRxiv a license to display the preprint in perpetuity. It is made available under a CC-BY-NC-ND 4.0 International license .

the loosening of the containment measures, thus maintaining the epidemic curve in the decreasing trajectory achieved during the lockdown (blue lines in Fig. 2). In analogy to the analyses presented above, we show results under the three different assumptions about the heavy symptomatic fraction: $\sigma = 50\%$, 25% and 10%.

Figure 4 also reports the estimated abundances of exposed, E, and individuals at peak infectivity, P, in the considered regions at the date of the announced new measures (May 4), along with the expected number of new daily symptomatic cases (C) predicted by the model. As an example, in Lombardia an increase in transmission of 40 % would lead to a rebound of the epidemic curve (Fig. 2). However, for the reference value of $\sigma = 25\%$, daily isolation of about ~1200 out of ~22 000 (~5.5 %) individuals belonging to the E and P compartments would effectively counterbalance the increase in transmission and bring back the curve to the baseline scenario (blue curve in Fig. 2). The reported isolation target in terms of the number of individuals to be isolated (left axis of Fig. 4) refers to the necessary effort right after the relaxation of the containment measures. If the epidemic is successfully controlled, and the cases continue to decline (i.e. they follow the baseline scenario), the isolation effort proportionally decreases over time. The isolation effort in terms of percentage of E and P individuals to be isolated (right axis of Fig. 4) remains instead constant.

While the isolation effort expressed as percentage of the E and P individuals to be isolated daily is not particularly sensitive to the assumed fraction of infections developing heavy symptoms, σ, the value changes dramatically when expressed in terms of the absolute number of individuals (Fig. 4). As σ decreases, a larger fraction of the epidemic remains unobserved. Therefore, to closely match the daily hospitalizations data, a much larger pool of E and P individuals is estimated (Fig. 4).

To assess the feasibility of the isolation effort required to contain the epidemic, we report the amount that can be achieved by tracing and isolating all the infections generated by the new daily symptomatic cases (black dashed lines in Fig. 4). For a given increase in transmission, a required effort (solid lines in Fig. 4) exceeding such amount implies that tracing and isolation of all primary infections generated by the new daily symptomatic cases is insufficient. In this case, secondary infections (i.e. infections generated by the primary infectees) need also to be targeted. As the role of the unobserved epidemic increases (i.e. σ decreases, from left to right columns in Fig. 4), isolation of primary contacts alone can compensate only for mild increases in transmission.

The timing of the relaxation of the restrictive measures also has a great impact on the isolation effort required to control the epidemic. Delaying the release of containment measures by an additional month would have reduced the abundance of E and P individuals by about two thirds, thus proportionally reducing the number of individuals that need be isolated (Fig. S7).

medRxiv preprint doi: https://doi.org/10.1101/2020.04.30.20083568; this version posted May 12, 2020. The copyright holder for this preprint (which was not certified by peer review) is the author/funder, who has granted medRxiv a license to display the preprint in perpetuity. It is made available under a CC-BY-NC-ND 4.0 International license .

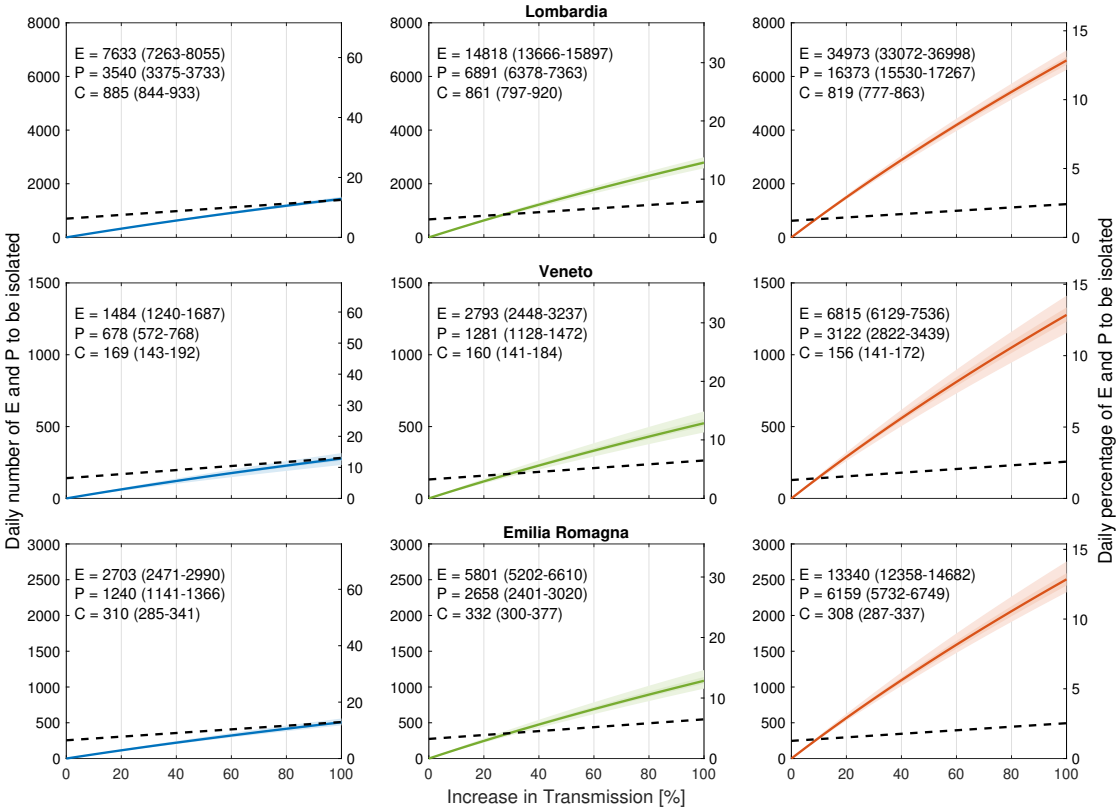

Figure 4: Daily number (left axis) and daily percentage (right axis) of exposed E and individuals at peak infectivity, P, to be isolated daily to maintain the epidemic trajectory onto the blue curve in Fig. 2 (corresponding to the current lockdown) despite the possible increase in transmission induced by the actual release of restrictions (horizontal axes). Different columns refer to different values of the symptomatic fraction σ: 50% (left, blue), 25% (center, green) and 10% (right, red). Solid lines refer to median values, shaded areas the 95 % (lighter shade) and 50 % confidence intervals. In each panel, median and 95 % confidence interval of E, P and new daily symptomatic cases (C) are given (estimates refer to May 4). The dashed black lines indicate the estimated number of E and P individuals that can be isolated by tracing all the infections generated by the new daily symptomatic cases. The other Italian regions are shown in Supplementary Figures S4, S5 and S6.

medRxiv preprint doi: https://doi.org/10.1101/2020.04.30.20083568; this version posted May 12, 2020. The copyright holder for this preprint (which was not certified by peer review) is the author/funder, who has granted medRxiv a license to display the preprint in perpetuity. It is made available under a CC-BY-NC-ND 4.0 International license .

Discussion

The above results, whose reliability to issue scenarios stems from their capability to closely match the hospitalization data locally and globally, probed in particular the role of inapparent infections by assuming a rather broad range of values of σ. The highest value ($\sigma = 50\%$) matches the empirical results found by testing for two weeks an entire community (Vo' Euganeo, IT, $\sim$ 3000 inhabitants)[10], whereas the lowest ($\sigma = 10\%$) is likely to be a lower bound, unachievable in the actual geographic context, because it may reflect also the age structure of a much younger population[35]. Another way to assess the plausibility of the assumed fraction of infections that develop heavy symptoms, is to compare the IFR estimated with different values of σ. The values of IFR corresponding to $\sigma = 25\%$ and $\sigma = 10\%$ (2% and 0.8%, respectively) bracket the available estimates of IFR for western countries[36]. Thus the median value assumed ($\sigma = 25\%$) seems like a sensible choice to probe the actual role of the unobserved epidemics in Italy.

Social distancing, PPE use, reduced or impeded mobility, and increased awareness led to an overall decrease of transmission of about 65% with respect to the initial uncontrolled epidemic (Fig. 1d). This result is consistent with other estimates obtained using different methods[37,38], and is largely attributable to the implemented measures, and only marginally to acquired immunity. Indeed, even in the most extreme scenario considered here ($\sigma = 10\%$), the acquired immunity would be responsible for less than 15% of the reduction occurred in the most severely hit region (Lombardia, Fig. 4), suggesting that herd immunity is far even in the hardest hit territories and. Seasonality effects[5], not explicitly accounted for here, might also have had a role in the reduction of transmission.

The scenarios shown in Fig. 2 suggest the impact of social distancing, testing, contact tracing and household quarantine on a possible second-wave of the COVID-19 epidemic in Italy (see also[34]). Actually, an observed deviation of incoming data from the baseline in Fig. 2 (say, towards an unacceptable epidemic trajectory like the purple curve) should raise a red flag and call for control action. Matching the right scenario in real time may be achieved through data assimilation and ensemble Kalman filtering[8]. The continuous update of the estimated state and parameters of the system, in fact, would allow the coupling of feedback and feed-forward controls, thus projecting the number of apparent and inapparent infections at least a latency period ahead of time. Incidentally, we deem this feature a significant advance produced by our method. Indeed, this procedure would provide – in time for action – a reasoned assessment of the actual exposure, in particular the number of exposed and infectious individuals that only models can evaluate. This is tantamount to distinguishing, after lifting the lockdown, between potential and realized transmission. The former is the maximum possible prevention of contagion given a set of rules. The latter is the bulk effect of the effective compliance to precautions associated with the relaxation of the lockdown. Thus, an increase in estimated exposure reflects the actual collective behaviors of mobile individuals, and the collective respect of rules

medRxiv preprint doi: https://doi.org/10.1101/2020.04.30.20083568; this version posted May 12, 2020. The copyright holder for this preprint (which was not certified by peer review) is the author/funder, who has granted medRxiv a license to display the preprint in perpetuity. It is made available under a CC-BY-NC-ND 4.0 International license .

regarding social distancing, PPE adoption, or crowding, to name a few. We argue that realized transmission can only be evaluated from early signs decoded from scenarios implemented through a model akin to ours.

Control may consist in either re-tightening of the containment measures, possibly of the stop-and-go type[5], or alternative interventions. While the strategy adopted during the first phase of the outbreak mostly relied on the isolation and treatment of symptomatic cases, a different mix of interventions is possible and desirable for the second phase. A keystone of such a mix should be an increased isolation effort by tracing[39] and testing[32] individuals who have been in close contact with a known infection[24,40], possibly with the help of technological advances like tracing apps[33].

We estimated the isolation target needed to counterbalance an increase in effective transmission (Fig. 4), and to maintain the epidemic trajectory onto the decreasing pattern achieved during lockdown. One way to achieve the required isolation target is to trace the close contacts of daily new symptomatic cases, who are more likely to self-report or be otherwise identified. However, as infected individuals might not immediately test positive, and because obtaining test results takes time, this strategy might imply as a matter of precaution to isolate, at least temporarily, all close contacts that the symptomatic case has had in the previous days. Tracing and isolating all primary infections generated by the symptomatic cases is a challenging task, because tracing is hardly exhaustive and not all symptomatic cases can be identified. Depending on the extent of the unobserved epidemic, however, isolation of primary infections might not suffice (see Fig. 4). Secondary contacts ought to be targeted as well in this case. Testing primary contacts would help identifying actually infected cases, thus refining the tracing of secondary contacts[32]. We also showed that, if the isolation target proves impossible to achieve for the limits of resources and/or logistical reasons, a possible strategy may consist in delaying further relaxations of confinement measures. Our results thus suggest that each Italian region should carefully evaluate its current strategies for tracing, testing and its isolation capacity, to plan and manage the second phase of the epidemic.

To keep the epidemic under control, health policy makers should consider a mix of interventions that include the re-tightening of confinement measures, possibly by a stop-and-go implementation based also on seasonality effects, or evidence on limits to the acquired immunity[5], and/or the effective isolation of infectious individuals[4,8]. Modeling studies can provide reasoned estimates of the minimum target to be attained, in this study through the latters. The proper strategy to achieve the isolation target is the domain of public health policy. The complementary use of testing in the control strategy is instead the domain of virology and epidemiology. To both domains, proper modelling scenarios offer information otherwise unavailable.

medRxiv preprint doi: https://doi.org/10.1101/2020.04.30.20083568; this version posted May 12, 2020. The copyright holder for this preprint (which was not certified by peer review) is the author/funder, who has granted medRxiv a license to display the preprint in perpetuity. It is made available under a CC-BY-NC-ND 4.0 International license .

Methods

Epidemiological model

The original $SEPIA$ model

Here, we use the model $SEPIA$[9]. The model is spatially explicit, i.e. it accounts for the coupled dynamics of a set of n interacting communities. In each community, say i ($i = 1 \ldots n$), the model includes the following compartments: Susceptible (S_i), Exposed (E_i), Peak infectivity (P_i), Infected with heavy symptoms (I_i), Asymptomatic/mildly symptomatic (A_i), Hospitalized (H_i), Quarantined at home (Q_i), Recovered (R_i), and Dead (D_i) individuals. The dynamics of transmission is given by:

$$\begin{aligned}
\dot{S}_i &= -\lambda_i(t) S_i \\
\dot{E}_i &= \lambda_i(t) S_i - \delta_E E_i \\
\dot{P}_i &= \delta_E E_i - \delta_P P_i \\
\dot{I}_i &= \sigma \delta_P P_i - (\eta + \gamma_I + \alpha_I) I_i \\
\dot{A}_i &= (1-\sigma)\delta_P P_i - \gamma_A A_i \\
\dot{H}_i &= (1-\zeta)\eta I_i - (\gamma_H + \alpha_H) H_i \\
\dot{Q}_i &= \zeta \eta I_i - \gamma_Q Q_i \\
\dot{R}_i &= \gamma_I I_i + \gamma_A A_i + \gamma_H H_i + \gamma_Q Q_i \\
\dot{D}_i &= \alpha_I I_i + \alpha_H H_i \,.
\end{aligned} \tag{1}$$

Susceptible individuals (S_i) become exposed to the viral agent by contacting individuals who are in any of the three infectious stages, namely peak infectivity, heavily symptomatic or asymptomatic/mildly symptomatic. Frequency-dependent contact rates are assumed, so that exposure is governed by the community-dependent, time-varying force of infection

$$\lambda_i(t) = \sum_{j=1}^{n} C^S_{ij}(t) \frac{\sum_{Y\in\{P,I,A\}} \sum_{k=1}^{n} \beta_{Y,k}(t) C^Y_{kj}(t) Y_k}{\sum_{X\in\{S,E,P,I,A,R\}} \sum_{k=1}^{n} C^X_{kj}(t) X_k} \,,$$

where $C^X_{ij}(t)$ (with $X \in \{S, E, P, I, A, R\}$) is the probability ($\sum_{j=1}^{n} C^X_{ij}(t) = 1$ for all i's, X's, and t's) that individuals in epidemiological state X who are from community i enter into contact with individuals who are present at community j at time t as either residents or because they are traveling there from community k (note that i, j and k may coincide), and $\beta_{Y,j}(t)$ ($Y \in \{P, I, A\}$) are the stage- and time-dependent transmission rates.

Exposed individuals (E_i) are latently infected, until they enter the peak infectivity stage (at rate δ_E). This stage has been specifically introduced[9] to account for the

medRxiv preprint doi: https://doi.org/10.1101/2020.04.30.20083568; this version posted May 12, 2020. The copyright holder for this preprint (which was not certified by peer review) is the author/funder, who has granted medRxiv a license to display the preprint in perpetuity. It is made available under a CC-BY-NC-ND 4.0 International license .

clinical and epidemiological evidence indicating that viral shedding peaks just before symptom onset and then declines after the emergence of symptoms or the evolution towards an asymptomatic case[10,13]. Peak infectivity individuals (P_i) progress (at rate δ_P) to become (with probability σ) either symptomatic individuals with heavy clinical symptoms (I_i) or (with probability $1-\sigma$) asymptomatic/mildly symptomatic individuals (A_i). Heavily symptomatic infectious individuals exit their compartment if/when (a) they seek treatment at a health-care facility, (at rate η), following which they may be hospitalized (a fraction $1-\zeta$) or quarantined at home (a fraction ζ; either ways, they are assumed to be effectively removed from the general community), (b) recover from infection (at rate γ_I), or (c) die (at rate α_I). Asymptomatic/mildly symptomatic individuals (A_i) leave their compartment upon recovering from infection (at rate γ_A). Hospitalized individuals (H_i) may either recover from infection (at rate γ_H) or die (at rate α_H). Quarantined (i.e. home-isolated) individuals (Q_i) leave their compartment upon recovery (at rate γ_Q). People recovering from infection or dying because of COVID-19 populate the classes of recovered (R_i) and dead (D_i) individuals, respectively.

Application of the model to the Italian COVID-19 epidemic

Model (1) is run at the scale of second-level administrative divisions, i.e. provinces and metropolitan cities (107 units as of 2020). Population size in each spatial unit is taken from the official estimates provided yearly (last update: January 1st, 2019) by the Italian National Institute of Statistics (Istituto Nazionale di Statistica, ISTAT; data available at `http://dati.istat.it/Index.aspx?QueryId=18460`).

The values of the transmission rates ($\beta_{Y,i}(t)$) are dependent on epidemiological status ($Y \in \{P, I, A\}$) as in the original formulation of the model[9]. In addition, they are assumed to be space- and time-dependent to take into account the effects of the various containment measures put in place in the first months of the epidemic (see below for further details).

Spatial coupling is parameterized by using information from the latest nation-wide assessment of mobility fluxes, which was produced by the Italian National Institute of Statistics (ISTAT) in 2011 (data available at `https://www.istat.it/it/archivio/139381`). For each second-level administrative unit (province), say i, two quantities are extracted from the ISTAT data, namely the fraction p_i of mobile people, i.e. the residents of i who defined themselves as commuters, and the fraction q_{ij} of mobile people between i and all other administrative units $j = 1 \ldots n$ (including $j = i$). The contact probabilities at the beginning of the epidemic ($t = 0$), $C^X_{ij}(0)$ ($X \in \{S, E, P, I, A, R\}$) are then defined based on the quantities p_i and q_{ij}. Specifically, we assume

$$C^X_{ij}(0) = \begin{cases} (1-p_i) + (1-r_X)p_i + r_X p_i q_{ij} & \text{if } i = j \\ r_X p_i q_{ij} & \text{otherwise}, \end{cases}$$

medRxiv preprint doi: https://doi.org/10.1101/2020.04.30.20083568; this version posted May 12, 2020. The copyright holder for this preprint (which was not certified by peer review) is the author/funder, who has granted medRxiv a license to display the preprint in perpetuity. It is made available under a CC-BY-NC-ND 4.0 International license .

where the parameter r_X ($0 \leq r_X \leq 1$) describes the fraction of contacts occurring while individuals in epidemiological compartment X are traveling. In other words, for community i, the social contacts of non-mobile people (a fraction $1 - p_i$ of the community size), those of mobile people that do not occur during travel (a fraction $1 - r_X$ of total contacts for people in epidemiological compartment X) and those associated with mobility for people who travel within their community (a fraction q_{ii} of mobile people) contribute to social mixing within the community. Conversely, the contacts occurring between two different communities, say i and j, are a fraction r_X of the total contacts of the individuals in epidemiological compartment X, multiplied by the probability p_i that people from i travel (independently of the destination) and the probability q_{ij} that the travel occurs between i and j. To account for the effect of the confinement measures, we progressively reduce extra province mobility according to the estimates obtained through the analysis of data collected through mobile applications[23]. As a conservative assumption, we elaborate near future scenarios maintaining the same level of extra-province mobility estimated during the lockdown, as only few commercial and production activities have resumed and extra-regional mobility is not allowed.

Epidemiological data

For the calibration of the model we consider the epidemiological data collected by the Dipartimento della Protezione Civile (data available at `https://github.com/pcm-dpc/COVID-19`), which are released daily and comprehend: at the regional level, the cumulative numbers of positive, dead and recovered individuals, together with the actual number of positive individuals that hospitalized or are under quarantine at home; at the province level, the cumulative numbers of positive cases.

Due to the strong space-time variations in the number of tests performed, the most trustworthy variable to monitor the outbreak is the daily number of hospitalizations, in the following indicated with H^{in}. This quantity corresponds to the flux $(1 - \zeta)\eta I$ in the H compartment of our model, and grants a straightforward link between data and model variables. However, H^{in} is not directly provided in the online data, and we thus adopt a stochastic approach to derive H^{in} combining data regarding the number of hospitalized individuals and deaths, and estimated distribution of delays between hospitalization and death or discharge.

At any given day k, H_k^{in} is obtained by the observed variations in the daily number of hospitalized individuals, $H_k - H_{k-1}$, plus the daily deaths $D_k^{\text{out}} = D_k - D_{k-1}$, and the number of individuals discharged from the hospital, here indicated with R_k^{out}. Under the assumption that the recorded deaths for COVID-19 are all from the hospitals, R_k^{out} is obtained by modeling as random variables the days τ spent in a hospital before death, whose probability density function (PDF) is indicated with $p_D(\tau)$, and the time in a hospital before discharge, whose PDF is indicated with $p_R(\tau)$.

Our procedure consists of the following steps. Sampling a random value from $p_D(\tau)$

medRxiv preprint doi: https://doi.org/10.1101/2020.04.30.20083568; this version posted May 12, 2020. The copyright holder for this preprint (which was not certified by peer review) is the author/funder, who has granted medRxiv a license to display the preprint in perpetuity. It is made available under a CC-BY-NC-ND 4.0 International license .

for each individual in D^{out}, we obtain the days of entrance of individuals that will die, thus the sequence D_k^{in}. We estimate the number of individuals entering on day k that will be eventually discharged as:

$$R_k^{\text{in}} = H_k^{\text{in}} - D_k^{\text{in}}$$

Then R_k^{out} is obtained by sampling an exit time from $p_R(\tau)$ for each individual in R_k^{in}. Finally:

$$H_k^{\text{in}} = H_k - H_{k-1} + D_k^{\text{out}} + R_k^{\text{out}}.$$

Reports by ISS indicate that for COVID-19 casualties the median residence time at a hospital is about 8 days for patients that accessed ICU, and 5 days without ICU[41]. We use this information to parameterize the distribution $p_D(\tau)$ as a gamma distribution of mean 7 and coefficient of variation 0.5 (hence, a median of 6.42 days; 0.05–0.95 quantiles: 2.39–13.56 days). We also assume that $p_R(\tau)$ follows a gamma distribution of mean 14 and coefficient of variation 0.5, which has a median of 13.7 days (0.05–0.95 quantiles: 4.78–27.14 days), in agreement with the recovery rate previously estimated[9].

Final data adopted for parameter estimation of the regional model is the median over 100 random generations of H_k^{in}, downscaled to the province level and smoothed by using a moving average of 7 days. A sensitivity analysis of H_k^{in} on the parameters of the $p_D(\tau)$ and $p_R(\tau)$ showed that the time series considered have only marginal variations.

Parameter estimation

The effect of the containment measures was parameterized in our previous application[9] by assuming that the transmission parameters (β_P, β_I and β_A) had a sharp decrease after the containment measures announced on February 24 and March 8. We update here such description to fully account for the set of progressively more restrictive measures that were introduced form March 8 to March 22, when also non-essential industrial and production activities were stopped. We describe the temporal changes in the β_P's (the remaining transmission parameters, β_I and β_A, are assumed to be proportional to β_P, see table 1) using 4 values: The value before February 24 (β_{P_0}), the values achieved right after (within two days) the measures introduced on February 24 (β_{P_1}) and the first set of lockdown measures implemented on March 8 (β_{P_2}). Finally, we assume that due to the progressive implementation of the lockdown and the introduction of more restrictive measures, the transmission rates further linearly decreased from March 10 to March 22, eventually achieving the value (β_{P_3}), which is then held constant. We let β_{P_3} vary among different Italian regions to reflect possible heterogeneity in disease transmission. Specifically, we estimate the hyperparameters controlling the prior of the parameters β_{P_3}/β_{P_2} (a Gaussian distribution truncated between 0 and 1) in a hierarchical Bayesian framework.

medRxiv preprint doi: https://doi.org/10.1101/2020.04.30.20083568; this version posted May 12, 2020. The copyright holder for this preprint (which was not certified by peer review) is the author/funder, who has granted medRxiv a license to display the preprint in perpetuity. It is made available under a CC-BY-NC-ND 4.0 International license .

Parameter	(units)	**Median**	95 % CI	**Information**
β_{P_0}	(d^{-1})	1.26	[1.24, 1.28]	Estimated
$1/\delta_E$	(d)	4.6		[13,24]
$1/\delta_P$	(d)	2		[13,24]
$1/\eta$	(d)	5		[44]
$1/\gamma_I$	(d)	14		[9]
$1/\alpha_I$	(d)	25		[9]
β_A/β_P	(1)	0.022	[0.020, 0.030]	Estimated
β_I/β_A	(1)	1		[9,10]
β_{P_1}/β_{P_0}	(1)	0.89	[0.87, 0.92]	Estimated
β_{P_2}/β_{P_1}	(1)	0.72	[0.70, 0.73]	Estimated
mean β_{P_3}/β_{P_2}	(1)	0.50	[0.48, 0.51]	Estimated
standard deviation β_{P_3}/β_{P_2}	(1)	0.038	[0.025, 0.053]	Estimated
Δt_0	(d)	35		[9]
ω	(1)	2.42	[2.33, 2.52]	Estimated

Table 1: Model parameters. The posterior distribution of the parameters marked as estimated was sampled through the DREAM_{ZS} implementation of the Markov chain Monte Carlo algorithm[45]. For all estimated parameters we used uninformative priors within biologically meaningful boundaries. Following our previous application[9], we assumed $\sigma = 0.25$, $r_S = 0.5$, $\zeta = 0.45$ and $r_E = r_P = r_A = r_R = r_S$, while $r_I = r_Q = r_H = 0$. Moreover: $\gamma_Q = \gamma_I = \gamma_H$, $\gamma_A = 2\gamma_I$, and $\alpha_H = \alpha_I$.

We impose an initial condition of one exposed individual in the province of Lodi (where the first cases were reported) Δt_0 days before February 24. Following our previous application[9], we estimate also the initial condition of the exposed compartment in each province to account for the possible seeding effect occurred during this period.

Parameters are estimated comparing data and simulation of the flux of hospital admissions ($(1-\zeta)\eta I$) at the provincial scale. We assume that each data point follows a negative binomial distribution with mean μ, equal to the value predicted by the model, and variance equal to $\omega\mu$ (NB1 parametrization[42,43]). Parameter values are summarized in Table 1.

The effect of testing and isolation

Following lockdown release, the expected increase in the transmission rates can be compensated by isolation of cases. Clinical and epidemiological evidence suggests that viral shedding peaks at the end of the latent period, and that shedding rapidly declines after the symptoms' onset or the evolution towards an asymptomatic case[13]. Moreover, viral shedding is similar regardless of the emergence of symptoms in the disease course

medRxiv preprint doi: https://doi.org/10.1101/2020.04.30.20083568; this version posted May 12, 2020. The copyright holder for this preprint (which was not certified by peer review) is the author/funder, who has granted medRxiv a license to display the preprint in perpetuity. It is made available under a CC-BY-NC-ND 4.0 International license .

of a patient[10]. This evidence suggests that isolation should be more effective if targeted at individuals in the exposed, E, and peak infectivity, P, compartments of the model. Therefore, we focus on these individuals as priority targets for isolation.

When isolation is enforced, two out-fluxes, $\rho_{E,i}E_i$ and $\rho_{P,i}P_i$, must be considered from the exposed and peak infectivity compartments, respectively. The parameters $\rho_{E,i}$ and $\rho_{P,i}$ (days^{-1}) represent the community-dependent rate at which infected individuals in the E_i and P_i classes are effectively isolated from the community. For the sake of simplicity, we assume $\rho_E = \rho_P = \rho$. Also, individuals isolated are simply removed from the community, without any further consideration of their clinical trajectories, which is deemed reasonable considering the relatively short timespan of the simulations performed here.

We estimate for each province the percentage (i.e. ρ_i) and the corresponding number of individuals ($\rho_i(E_i + P_i)$) that should be isolated daily to counterbalance the increase in transmission due to the loosening of containment measures, so as to maintain the same level of trasmissivity achieved during the lockdown. In analogy to the analyses presented above, we repeat the estimation of the isolation effort under the three different assumptions about the heavy symptomatic fraction: $\sigma = 25\%$, 50% and 10%.

References

1. World Health Organization. *Coronavirus disease (COVID-2019) situation reports* https://www.who.int/emergencies/diseases/novel-coronavirus-2019/situation-reports/ (2020).
2. The Center for Systems Science and Engineering. *Coronavirus COVID-19 Global Cases* https://arcg.is/0fHmTX (2020).
3. European Commission. *Joint European Roadmap towards lifting COVID-19 containment measures* https://ec.europa.eu/info/sites/info/files/communication_-_a_european_roadmap_to_lifting_coronavirus_containment_measures_0.pdf (2020).
4. Leung, K., Wu, J. T., Liu, D. & Leung, G. M. First-wave COVID-19 transmissibility and severity in China outside Hubei after control measures, and second-wave scenario planning: a modelling impact assessment. *The Lancet* **395,** 1382–1393. doi:10.1016/s0140-6736(20)30746-7 (Apr. 2020).
5. Kissler, S. M., Tedijanto, C., Goldstein, E., Grad, Y. H. & Lipsitch, M. Projecting the transmission dynamics of SARS-CoV-2 through the postpandemic period. *Science,* eabb5793. doi:10.1126/science.abb5793 (Apr. 2020).
6. Giordano, G. *et al.* Modelling the COVID-19 epidemic and implementation of population-wide interventions in Italy. *Nature Medicine.* doi:10.1038/s41591-020-0883-7 (Apr. 2020).

medRxiv preprint doi: https://doi.org/10.1101/2020.04.30.20083568; this version posted May 12, 2020. The copyright holder for this preprint (which was not certified by peer review) is the author/funder, who has granted medRxiv a license to display the preprint in perpetuity. It is made available under a CC-BY-NC-ND 4.0 International license .

7. Editor, T. Coronavirus: shared lessons on lifting lockdowns. *Nature* **581,** 581. doi:http://dx.doi.org/10.1038/d41586-020-01311-x.

8. Li, R. *et al.* Substantial undocumented infection facilitates the rapid dissemination of novel coronavirus (SARS-CoV2). *Science,* eabb3221. doi:10.1126/science.abb3221 (Mar. 2020).

9. Gatto, M. *et al.* Spread and dynamics of the COVID-19 epidemic in Italy: effects of emergency containment measures. *Proc. Natl. Acad. Sci. USA*. Published online April 23, 2020. doi:10.1073/pnas.2004978117 (2020).

10. Lavezzo, E. *et al.* Suppression of COVID-19 outbreak in the municipality of Vo, Italy. doi:10.1101/2020.04.17.20053157. medRxiv: 2020.04.17.20053157 (Apr. 18, 2020).

11. Luo, L., Liu, D., Liao, X., *et al.* Modes of contact and risk of transmission in COVID-19 among close contacts. doi:10.1101/2020.03.24.20042606. medRxiv: 2020.03.24.20042606 (Mar. 26, 2020).

12. Bi, Q., Wu, Y., Mei, S., *et al.* Epidemiology and Transmission of COVID-19 in Shenzhen China: Analysis of 391 cases and 1,286 of their close contacts. doi:10.1101/2020.03.03.20028423. medRxiv: 2020.03.03.20028423 (Mar. 27, 2020).

13. He, X. *et al.* Temporal dynamics in viral shedding and transmissibility of COVID-19. *Nature Medicine.* doi:10.1038/s41591-020-0869-5 (Apr. 2020).

14. Du, Z. *et al.* Serial Interval of COVID-19 among Publicly Reported Confirmed Cases. *Emerging Infectious Diseases* **26.** doi:10.3201/eid2606.200357 (June 2020).

15. Nishiura, H., Linton, N. M. & Akhmetzhanov, A. R. Serial interval of novel coronavirus (COVID-19) infections. *International Journal of Infectious Diseases* **93,** 284–286. doi:10.1016/j.ijid.2020.02.060 (Apr. 2020).

16. Ganyani, T. *et al.* Estimating the generation interval for COVID-19 based on symptom onset data. doi:10.1101/2020.03.05.20031815. medRxiv: 2020.03.05.20031815 (Mar. 8, 2020).

17. Holshue, M. L. *et al.* First Case of 2019 Novel Coronavirus in the United States. *New England Journal of Medicine* **382,** 929–936. doi:10.1056/nejmoa2001191 (Mar. 2020).

18. Hoehl, S. *et al.* Evidence of SARS-CoV-2 Infection in Returning Travelers from Wuhan, China. *New England Journal of Medicine* **382,** 1278–1280. doi:10.1056/nejmc2001899 (Mar. 2020).

medRxiv preprint doi: https://doi.org/10.1101/2020.04.30.20083568; this version posted May 12, 2020. The copyright holder for this preprint (which was not certified by peer review) is the author/funder, who has granted medRxiv a license to display the preprint in perpetuity. It is made available under a CC-BY-NC-ND 4.0 International license .

19. Rothe, C. *et al.* Transmission of 2019-nCoV Infection from an Asymptomatic Contact in Germany. *New England Journal of Medicine* **382,** 970–971. doi:10.1056/nejmc2001468 (Mar. 5, 2020).

20. Wölfel, R. *et al.* Virological assessment of hospitalized patients with COVID-2019. *Nature.* doi:10.1038/s41586-020-2196-x (Apr. 1, 2020).

21. Tang, B. *et al.* Estimation of the Transmission Risk of the 2019-nCoV and Its Implication for Public Health Interventions. *Journal of Clinical Medicine* **9,** 462. doi:10.3390/jcm9020462 (Feb. 2020).

22. Flaxman, S. *et al. Report 13: Estimating the number of infections and the impact of non-pharmaceutical interventions on COVID-19 in 11 European countries* tech. rep. (2020). doi:10.25561/77731. https://spiral.imperial.ac.uk:8443/handle/10044/1/77731.

23. Pepe, E. *et al. COVID-19 outbreak response: first assessment of mobility changes in Italy following lockdown* tech. rep. (COVID-19 Mobility Monitoring project, 2020). https://covid19mm.github.io/in-progress/2020/03/13/first-report-assessment.html (2020).

24. Cereda, D. *et al. The early phase of the COVID-19 outbreak in Lombardy, Italy* arXiv: 2003.09320v1 [q-bio.PE]. https://arxiv.org/abs/2003.09320v1.

25. Guzzetta, G. *et al.* Potential short-term outcome of an uncontrolled COVID-19 epidemic in Lombardy, Italy, February to March 2020. *Eurosurveillance* **25.** doi:10.2807/1560-7917.es.2020.25.12.2000293 (Mar. 2020).

26. Dipartimento della Protezione Civile. *COVID-19 Italia - Monitoraggio della situazione* https://arcg.is/C1unv (2020).

27. Dipartimento della Protezione Civile. *Emergenza Coronavirus: la risposta nazionale* http://www.protezionecivile.gov.it/attivita-rischi/rischio-sanitario/emergenze/coronavirus (2020).

28. Istituto Superiore di Sanità. *Coronavirus: ultimi aggiornamenti* https://www.epicentro.iss.it/coronavirus/aggiornamenti (2020).

29. Ciminelli, G. & Garcia-Mandicó, S. *COVID-19 in Italy: An analysis of death registry data* https://voxeu.org/article/covid-19-italy-analysis-death-registry-data (2020).

30. ISTAT. *Impatto dell'epidemia COVID-19 sulla mortalità totale della popolazione residente. Primo trimestre 2020* https://www.istat.it/it/files//2020/05/Rapporto_Istat_ISS.pdf (2020).

medRxiv preprint doi: https://doi.org/10.1101/2020.04.30.20083568; this version posted May 12, 2020. The copyright holder for this preprint (which was not certified by peer review) is the author/funder, who has granted medRxiv a license to display the preprint in perpetuity. It is made available under a CC-BY-NC-ND 4.0 International license .

31. World Health Organization. *Rational use of personal protective equipment (PPE) for coronavirus disease (COVID-19): interim guidance* https://apps.who.int/iris/handle/10665/331498 (2020).

32. Grassly, N. *et al. Report 16: Role of testing in COVID-19 control* Imperial College London. https://www.imperial.ac.uk/media/imperial-college/medicine/mrc-gida/2020-04-23-COVID19-Report-16.pdf (2020).

33. Ferretti, L. *et al.* Quantifying SARS-CoV-2 transmission suggests epidemic control with digital contact tracing. *Science,* eabb6936. doi:10.1126/science.abb6936. https://doi.org/10.1126/science.abb6936.

34. Aleta, A. *et al. Modeling the impact of social distancing, testing, contact tracing and household quarantine on second-wave scenarios of the COVID-19 epidemic* https://cosnet.bifi.es/wp-content/uploads/2020/05/main.pdf (2020).

35. Dowd, J. B. *et al.* Demographic science aids in understanding the spread and fatality rates of COVID-19. *medRXiv.* (31 March 2020). doi:10.1101/2020.03.15.20036293. https://doi.org/10.1101/2020.03.15.20036293 (Mar. 2020).

36. Ferguson, N. *et al. Report 9: Impact of non-pharmaceutical interventions (NPIs) to reduce COVID-19 mortality and healthcare demand* (Imperial College London, 2020). doi:10.25561/77482. http://hdl.handle.net/10044/1/77482.

37. Vollmer, M. *et al. Report 20: Using mobility to estimate the transmission intensity of COVID-19 in Italy: A subnational analysis with future scenarios* tech. rep. (2020). doi:10.25561/78677. https://www.imperial.ac.uk/mrc-global-infectious-disease-analysis/covid-19/report-20-italy/.

38. Guzzetta, G. *et al.* The impact of a nation-wide lockdown on COVID-19 transmissibility in Italy. arXiv: 2004.12338v1 [q-bio.PE] (Apr. 26, 2020).

39. Hellewell, J. *et al.* Feasibility of controlling COVID-19 outbreaks by isolation of cases and contacts. *The Lancet Global Health* **8,** e488–e496. doi:10.1016/s2214-109x(20)30074-7 (Apr. 2020).

40. Zhang, J. *et al.* Evolving epidemiology of novel coronavirus diseases 2019 and possible interruption of local transmission outside Hubei Province in China: a descriptive and modeling study. doi:10.1101/2020.02.21.20026328. medRxiv: 2020.02.21.20026328 (Feb. 23, 2020).

41. Palmieri, L. *et al. Caratteristiche dei pazienti deceduti positivi a COVID-19 in Italia* Istituto Superiore di Sanità. https://www.epicentro.iss.it/coronavirus/bollettino/Report-COVID-2019_29_aprile.pdf (2020).

medRxiv preprint doi: https://doi.org/10.1101/2020.04.30.20083568; this version posted May 12, 2020. The copyright holder for this preprint (which was not certified by peer review) is the author/funder, who has granted medRxiv a license to display the preprint in perpetuity. It is made available under a CC-BY-NC-ND 4.0 International license .

42. Cameron, A. C. & Trivedi, P. K. Econometric models based on count data. Comparisons and applications of some estimators and tests. *Journal of Applied Econometrics* **1,** 29–53. doi:10.1002/jae.3950010104 (Jan. 1986).

43. Lindén, A. & Mäntyniemi, S. Using the negative binomial distribution to model overdispersion in ecological count data. *Ecology* **92,** 1414–1421 (2011).

44. Task force COVID-19. *Epidemia COVID-19, Aggiornamento nazionale: 23 aprile 2020* Dipartimento Malattie Infettive e Servizio di Informatica, Istituto Superiore di Sanità. https://www.epicentro.iss.it/coronavirus/bollettino/Bollettino-sorveglianza-integrata-COVID-19_23-aprile-2020.pdf (2020).

45. Ter Braak, C. J. F. & Vrugt, J. A. Differential Evolution Markov Chain with snooker updater and fewer chains. *Statistics and Computing* **18,** 435–446. doi:10.1007/s11222-008-9104-9 (Oct. 2008).

Acknowledgments

EB, DP and AR acknowledge funding from Fondazione Cassa di Risparmio di Padova e Rovigo (IT) through its grant 55722 (April 2020).

Contributors

EB, MG and AR were responsible for conceiving the work. EB, DP and LM were responsible for numerical simulations and model parameter estimation. All authors were responsible for data analysis and statistics and writing the manuscript.

Competing interests

We declare no competing interests.

medRxiv preprint doi: https://doi.org/10.1101/2020.04.30.20083568; this version posted May 12, 2020. The copyright holder for this preprint (which was not certified by peer review) is the author/funder, who has granted medRxiv a license to display the preprint in perpetuity. It is made available under a CC-BY-NC-ND 4.0 International license .

Supplementary Information

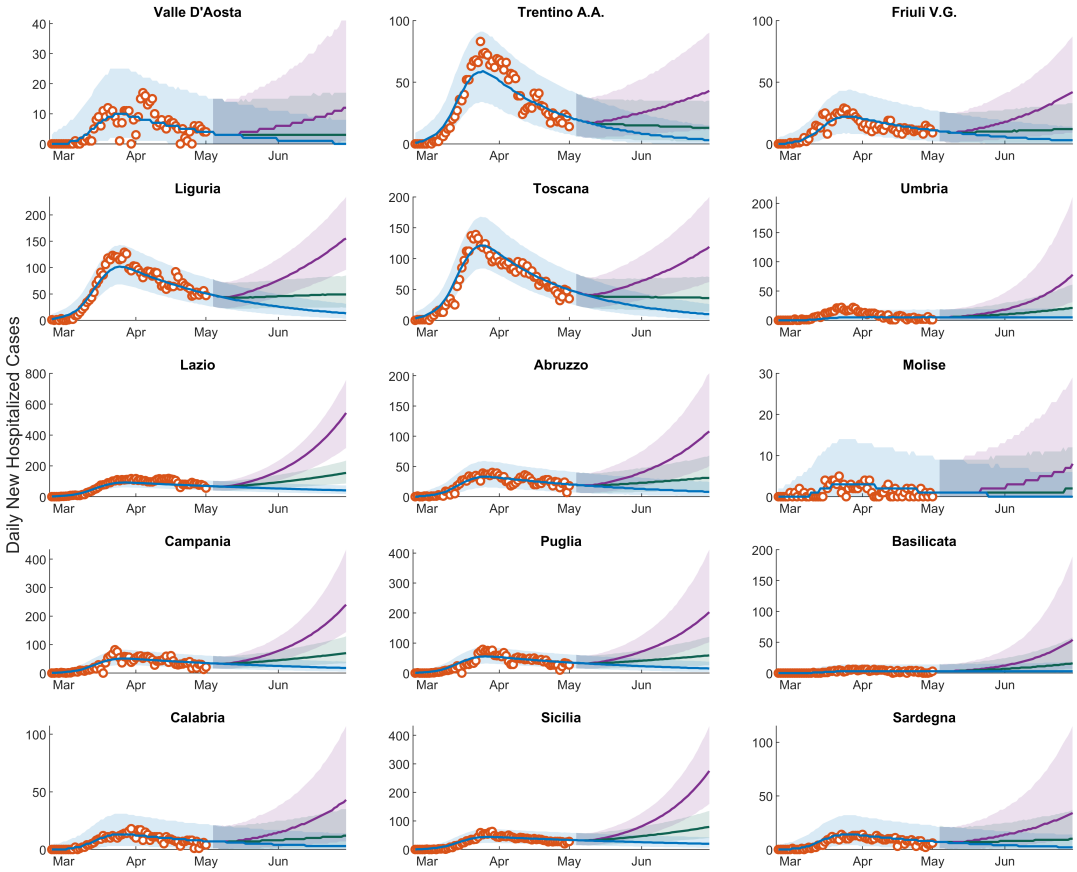

Figure S1: Epidemic scenarios for the regions not shown in Fig. 2.

medRxiv preprint doi: https://doi.org/10.1101/2020.04.30.20083568; this version posted May 12, 2020. The copyright holder for this preprint (which was not certified by peer review) is the author/funder, who has granted medRxiv a license to display the preprint in perpetuity. It is made available under a CC-BY-NC-ND 4.0 International license .

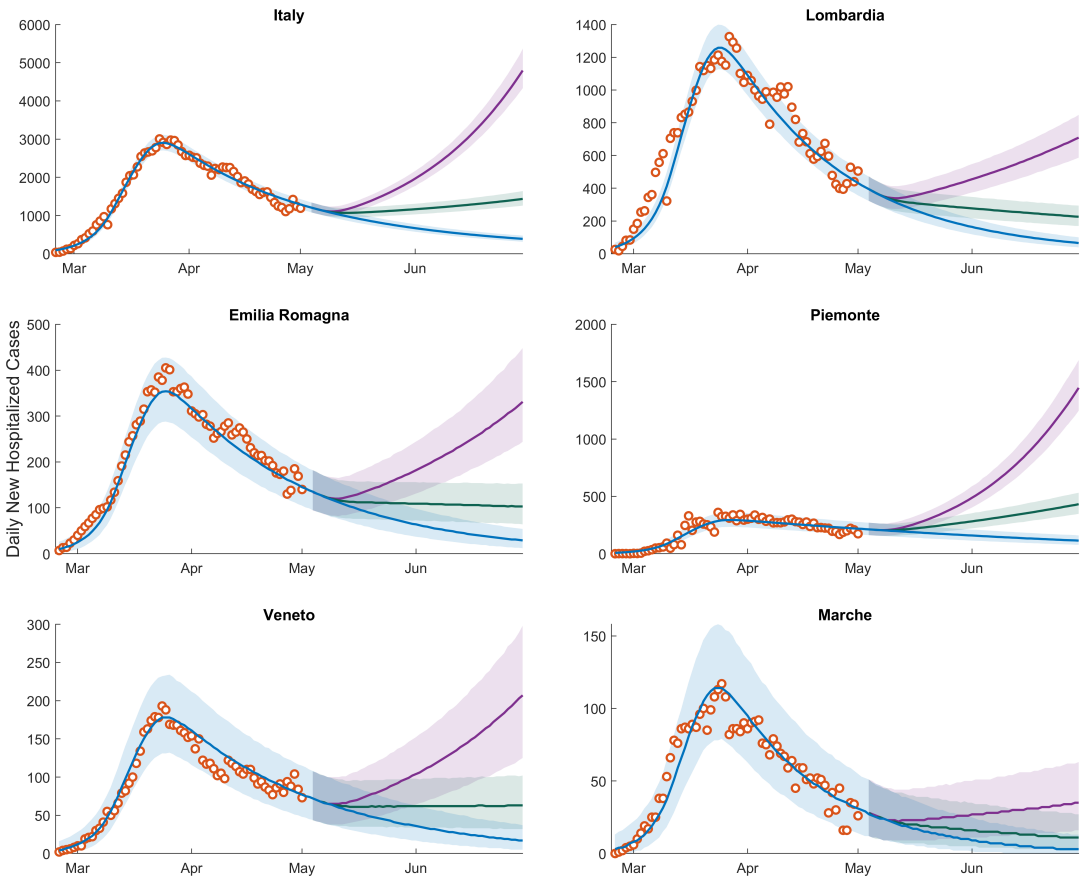

Figure S2: Same as Fig. 2 of the main text but for $\sigma = 50\%$

medRxiv preprint doi: https://doi.org/10.1101/2020.04.30.20083568; this version posted May 12, 2020. The copyright holder for this preprint (which was not certified by peer review) is the author/funder, who has granted medRxiv a license to display the preprint in perpetuity. It is made available under a CC-BY-NC-ND 4.0 International license .

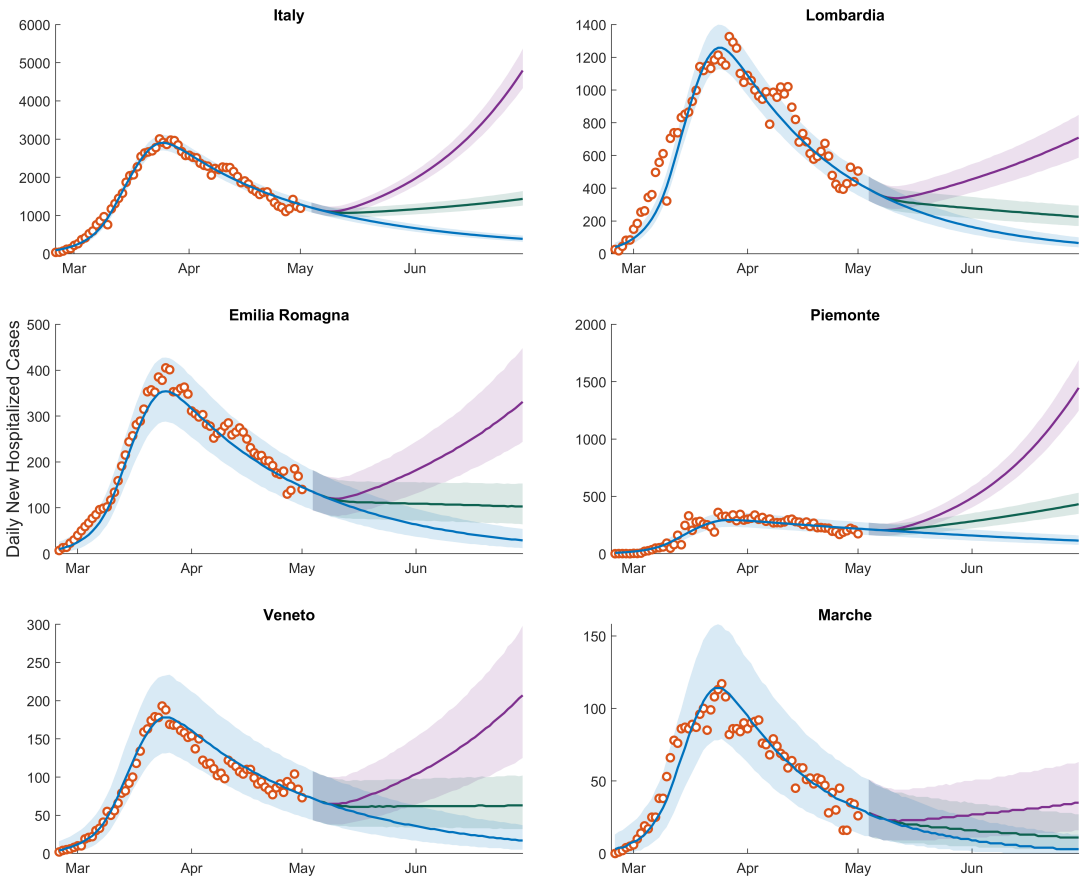

Figure S3: Same as Fig. 2 of the main text but for $\sigma = 10\%$

medRxiv preprint doi: https://doi.org/10.1101/2020.04.30.20083568; this version posted May 12, 2020. The copyright holder for this preprint (which was not certified by peer review) is the author/funder, who has granted medRxiv a license to display the preprint in perpetuity. It is made available under a CC-BY-NC-ND 4.0 International license .

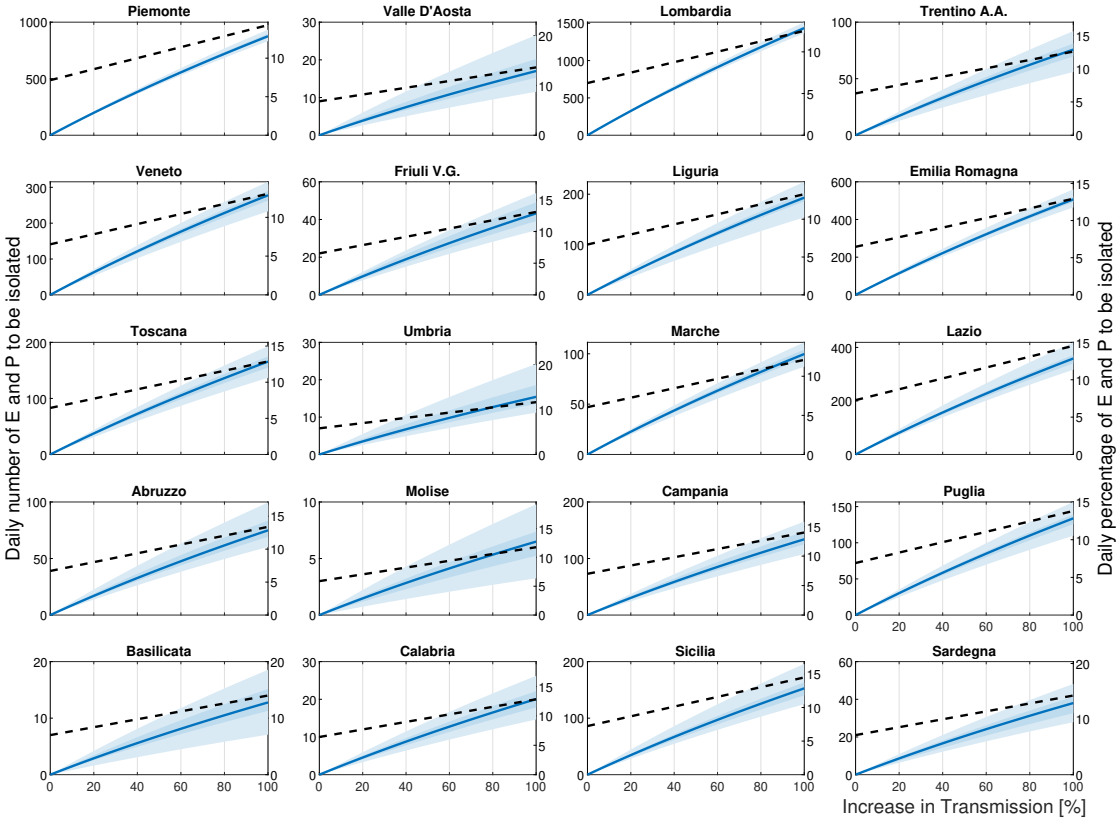

Figure S4: Isolation effort for all Italian regions. Symbols as in Fig. 4. Values refer to the case $\sigma = 50\%$.

medRxiv preprint doi: https://doi.org/10.1101/2020.04.30.20083568; this version posted May 12, 2020. The copyright holder for this preprint (which was not certified by peer review) is the author/funder, who has granted medRxiv a license to display the preprint in perpetuity. It is made available under a CC-BY-NC-ND 4.0 International license .

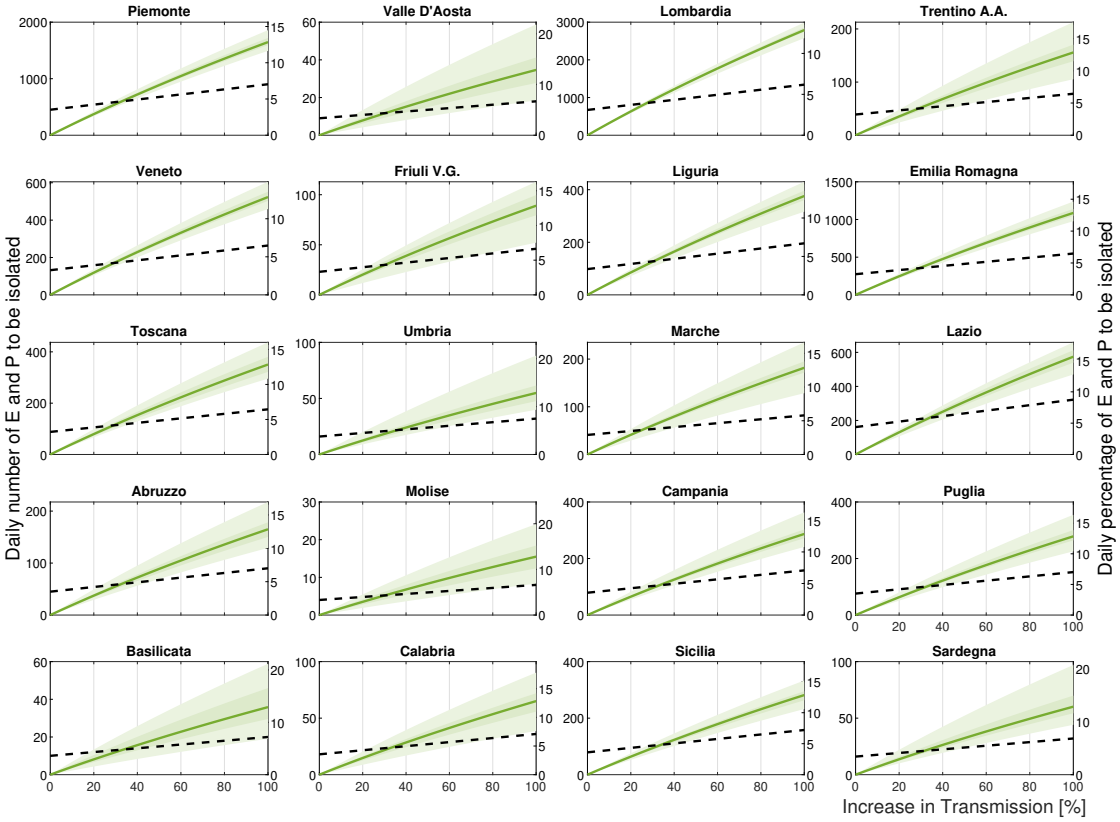

Figure S5: Isolation effort for all Italian regions. Symbols as in Fig. 4. Values refer to the case $\sigma = 25\%$.

medRxiv preprint doi: https://doi.org/10.1101/2020.04.30.20083568; this version posted May 12, 2020. The copyright holder for this preprint (which was not certified by peer review) is the author/funder, who has granted medRxiv a license to display the preprint in perpetuity. It is made available under a CC-BY-NC-ND 4.0 International license .

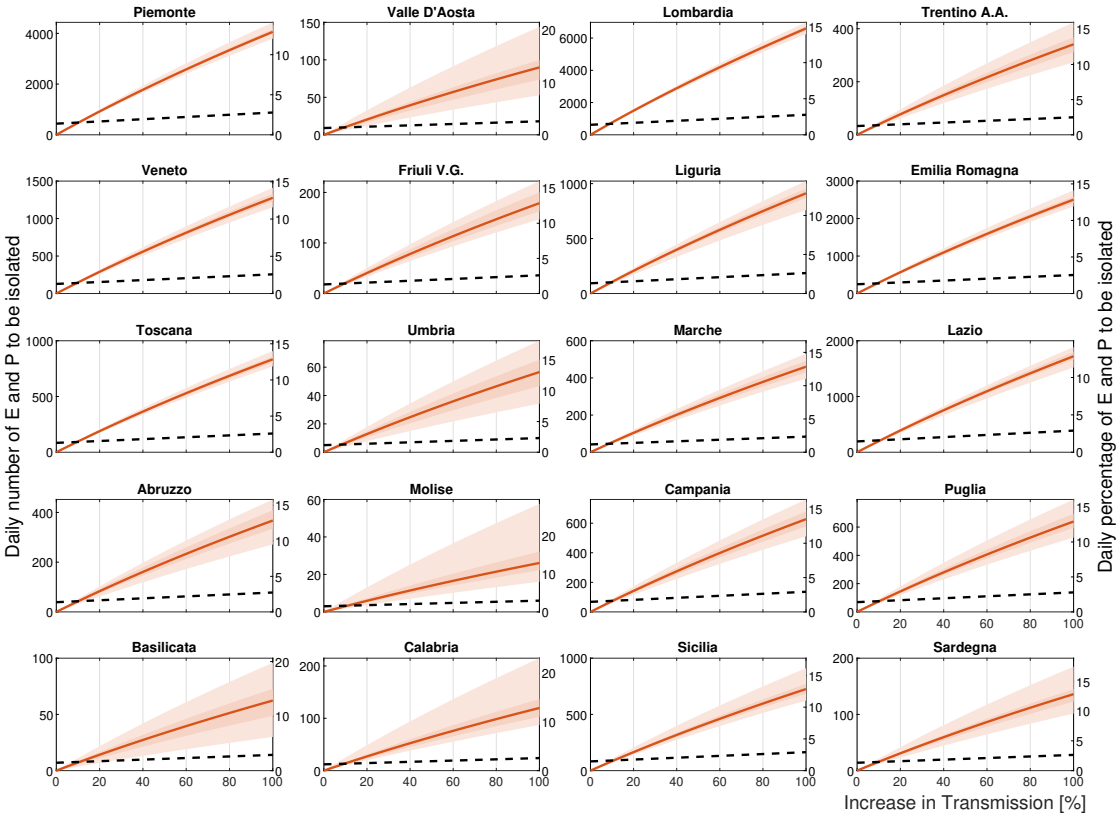

Figure S6: Isolation effort for all Italian regions. Symbols as in Fig. 4. Values refer to the case $\sigma = 10\%$.

medRxiv preprint doi: https://doi.org/10.1101/2020.04.30.20083568; this version posted May 12, 2020. The copyright holder for this preprint (which was not certified by peer review) is the author/funder, who has granted medRxiv a license to display the preprint in perpetuity. It is made available under a CC-BY-NC-ND 4.0 International license .

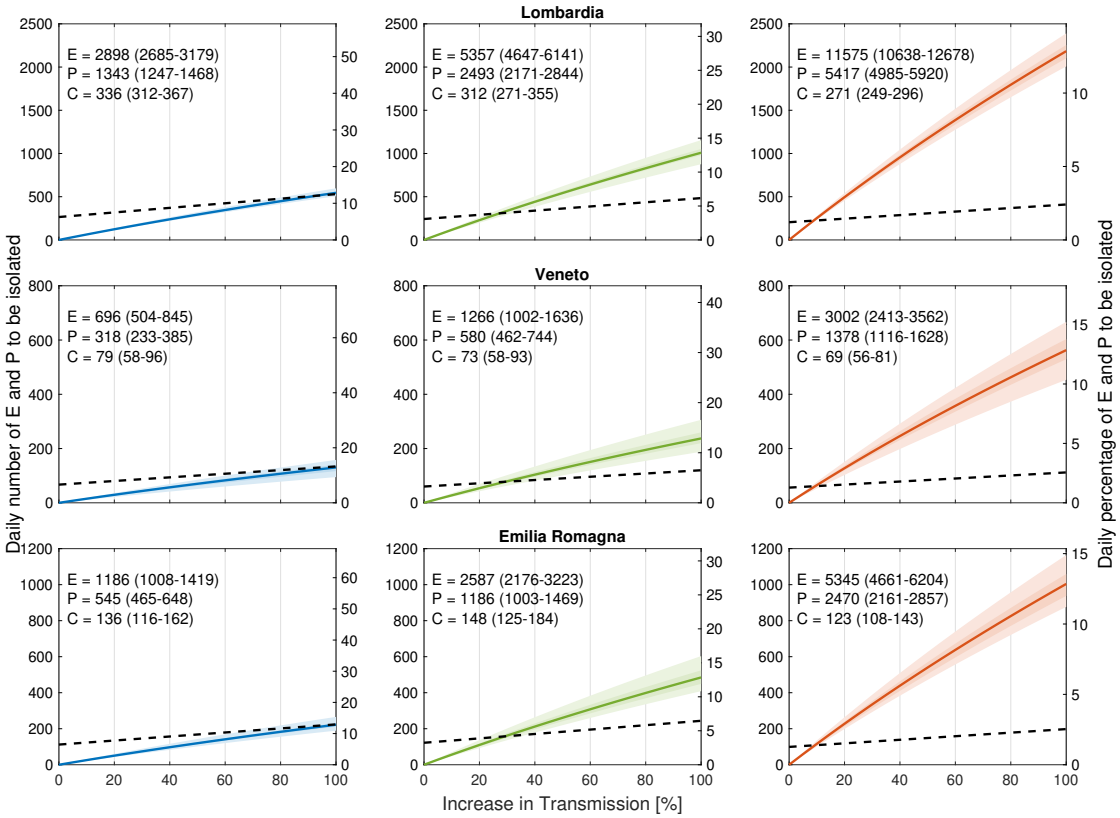

Figure S7: Isolation effort as shown in Fig. 4 but for a starting date of the relaxation of the restrictive measures delayed by one month.